

# Assessing Crash Risks of Evacuation Traffic: A Simulation-based Approach



**SAFETY RESEARCH USING SIMULATION**

**UNIVERSITY TRANSPORTATION CENTER**

Samiul Hasan, PhD  
Assistant Professor  
Department of Civil,  
Environmental and  
Construction Engineering  
University of Central Florida

Rezaur Rahman, MSc  
PhD Student  
Department of Civil,  
Environmental and  
Construction Engineering  
University of Central Florida

## **Assessing Crash Risks of Evacuation Traffic: A Simulation-based Approach**

Samiul Hasan, PhD  
Assistant Professor  
Department of Civil, Environmental and  
Construction Engineering  
University of Central Florida  
<https://orcid.org/0000-0002-5828-3352>

Rezaur Rahman, MSc  
PhD Student  
Department of Civil, Environmental and  
Construction Engineering  
University of Central Florida  
<https://orcid.org/0000-0002-0619-522X>

A Report on Research Sponsored by

SAFER-SIM University Transportation Center

Federal Grant No: 69A3551747131

December 2019

## *DISCLAIMER*

*The contents of this report reflect the views of the authors, who are responsible for the facts and the accuracy of the information presented herein. This document is disseminated in the interest of information exchange. The report is funded, partially or entirely, by a grant from the U.S. Department of Transportation's University Transportation Centers Program. However, the U.S. Government assumes no liability for the contents or use thereof.*

## Table of Contents

List of Figures .....	vi
List of Tables .....	vii
Abstract.....	viii
1 Introduction .....	9
1.1 Research Objectives and Contributions.....	11
2 Data Description and Exploration .....	13
2.1 Data Description .....	13
2.2 Data Exploration .....	14
3 Crash Risk Assessment During Evacuation .....	17
3.1 Data Preparation .....	17
3.2 Empirical Results.....	20
3.3 Summary.....	26
4 Microscopic Simulation of Evacuation Traffic.....	27
4.1 Data Preparation .....	27
4.2 Car-Following Model in SUMO .....	29
4.3 SUMO Simulation Model Development and Calibration .....	31
4.4 Surrogate Safety Measures .....	35
4.5 Simulation Results.....	37
4.6 Summary.....	40
5 Implications of the Research .....	42
6 Acknowledgments.....	43
References .....	44

## List of Figures

Figure 2.1 - Crash locations aggregated in an Open Street map based on the actual coordinates of the crashes .....	14
Figure 2.2 - Traffic flow variation in regular and evacuation period.....	16
Figure 2.3 - Number of crashes during Hurricane Irma evacuation.....	16
Figure 3.1 - Layout of the segments and MVDS detectors .....	18
Figure 3.2 - Pearson correlation values for different pairs of variables .....	23
Figure 4.1 - Study segment on I-75: (a) Google Map view of the route (b) Location of the MVDS detectors .....	28
Figure 4.2 - Variation of number of conflicts for different values of desired time headway.....	38
Figure 4.3 -Travel time variation at different market penetration rate of ACC vehicles.....	40

## List of Tables

Table 3.1 - Hazard ratios for the matched sample (sampling ratio for crash and non-crash is 1:5) .....	21
Table 3.2 - Hazard ratio for the final models for evacuation and regular period (sampling ratio for crash and non-crash is 1:5) .....	25
Table 3.3 – Coefficient estimates for unconditional logistic regression .....	26
Table 4.1 - Initial model before adjusting the parameters .....	30
Table 4.2 - Controller parameters for ACC .....	31
Table 4.3 - Parameter setting for model calibration .....	33
Table 4.4 - The final model after adjusting the parameters.....	35
Table 4.5 - Values of the performance metrics for the calibrated model .....	35
Table 4.6 - Percentage change in the number of conflicts averaged over 10 simulation runs (desired time headway is 1.3 sec) .....	39

## **Abstract**

Recently, hurricanes have caused major concern for transportation agencies and policymakers attempting to find better evacuation strategies. This was especially evident after Hurricane Irma, which forced about 6.5 million Floridians to evacuate the state. This mass evacuation caused a significant amount of delays on state highways due to heavy congestion and car crashes. Crashes and accidents on roads and highways are of major concern during evacuation efforts. Though several strategies have been implemented to manage the heavy traffic demand during a hurricane evacuation, current approaches seem to have less of an impact on traffic safety. In this context, this project had three objectives:

- To assess the impact of hurricane evacuation on crash risks,
- To identify if there are any changes in traffic flow behavior between evacuation and non-evacuation periods, and
- To assess the impact of an in-vehicle driving assistance system during an evacuation period.

First, to assess the impact of hurricane evacuation on crash risks, we adopted a matched case control approach. After collecting traffic and crash data along a major evacuation route in Florida, we estimated models for three different conditions: regular period, evacuation period, and a combination of both evacuation and regular period data. Model results show that if there is high occupancy at an upstream station and high variation of speed at a downstream station, the probability of crash occurrence increases. We estimate the effect of evacuation itself on crash risk and find that, after controlling for traffic characteristics, during evacuation the chance of an accident is higher than in a regular period. These findings will help us develop advanced real-time crash prediction models which will work for evacuation traffic conditions, and design proactive countermeasures to reduce crash occurrences during evacuation.

Second, to understand driver behavior during evacuation and to assess the potential safety impacts of adaptive cruise control (ACC) systems, we developed a microscopic simulation model in SUMO for a segment of the Interstate highway 75 (I-75), and calibrate it using real-world traffic data collected from the evacuation period of hurricane Irma. For the calibrated model, we find that the values of maximum acceleration and deceleration are  $4.5 \text{ m/s}^2$  and  $6.5 \text{ m/s}^2$ , respectively. These values are higher than those in typical car-following models calibrated under regular traffic conditions. Also, higher acceleration and deceleration values indicate abrupt speed variation, which is the most common scenario for evacuation traffic. To evaluate the safety impact of ACC systems, we adopted two surrogate measures: time to collision (TTC) and deceleration rate to avoid a collision (DRAC). Our experiment results show that during evacuation, about 49% of traffic collisions can be reduced at a 25% market penetration of ACC-equipped vehicles.

The findings from this project have further implications for evacuation declarations and highlight the need for better traffic management strategies during evacuation. Based on the findings, we propose several traffic management strategies to reduce the number of crashes during evacuation. We also propose solutions based on in-vehicle driving assistance systems and identify the challenges to increase market penetration rate for such technologies.

## **1 Introduction**

Devastating experiences from recent hurricanes such as Harvey, Irma, Maria, Florence, and Michael have made emergency evacuation a major issue for the coastal residents of the United States. For example, during Hurricane Irma in Florida, about 6.5 million residents were ordered to evacuate, causing significant traffic congestion and delay on two major highways (I-75 and I-95). Evacuation creates a surge in traffic demand resulting in irregular traffic flow patterns, which may cause traffic crashes. In such critical situations, it is a challenge for transportation agencies to ensure safe and efficient evacuation of a

large number of people. Several strategies have been deployed to manage high traffic volume during evacuation (1). However, these strategies seem to be less effective in reducing the number of traffic crashes.

During the evacuation period of Hurricane Irma, about 221 crashes occurred on I-75 from September 6 to September 9, 2017 (before the landfall day), causing significant delays for evacuees. Despite the high number of crashes, studies related to evacuation traffic modeling and safety analysis inadequately address the severity of this problem. To ensure the safe and efficient evacuation of a large number of people, it is necessary to assess the contributing factors which cause an increase in the number of crashes during evacuation.

During an evacuation period, traffic stream follows oscillatory speed, similar to a stop and go wave, potentially contributing to rear-end crashes (2–4). Previous studies have shown that in a stop and go traffic condition, rear-end collisions are the primary collision type, occurring due to frequent acceleration and deceleration induced by the propagation of kinematic waves (5–7). Also, the most dangerous situation occurs when the leading vehicle is forced to deaccelerate while the following vehicle maintains high speed (8–10). Li et al. (7) found that rear-end collisions in stop and go traffic depends on three parameters: perception-reaction time, initial gap between vehicles, and deceleration ability. These factors largely depend on the driver's perception of traffic condition. In hurricane evacuation—when evacuees are eager to reach a safe destination and are frustrated by dealing with heavily congested highways for hours—perception-related errors are inevitable. Thus, unstable traffic flow leading to driver perception error may contribute to a high number of collisions during a hurricane evacuation.

To reduce the number of crashes during evacuation, we cannot rely solely on infrastructure-based solutions. It is also necessary to implement advanced traffic management strategies that will improve traffic stability and provide route guidance and assistance to drivers. Strategies such as contraflow to facilitate evacuation traffic or the

use of hard shoulder as an extra lane to increase roadway capacity may help in reducing the number of traffic crashes. However, these strategies will not address and improve an evacuee's perception-related errors that may lead to traffic crashes. In such cases, in-vehicle driving assistance systems could be a viable solution.

### 1.1 Research Objectives and Contributions

To assess the crash risks of evacuation traffic and identify potential solutions, this project had three objectives:

- To assess the impact of hurricane evacuation on crash risks,
- To identify if there are any changes in traffic flow behavior between evacuation and non-evacuation periods, and
- To assess the impact of an in-vehicle driving assistance system during an evacuation period.

In this report, we present the data, method, and results of our investigation of the above objectives related to evacuation traffic. We first investigated the relationship between traffic state variables and crash occurrence at a macroscopic level. We also investigated whether evacuation itself has any influence on the increase in number of crashes. To understand driver behavior during evacuation, we designed a microsimulation approach and further investigated the influence of in-vehicle driving assistance system, such as adaptive cruise control (ACC), to reduce crash risks.

This project has made several contributions:

- i. Combining data from multiple sources to create a database that helps us gain insights on crash risk of evacuation using real-world hurricane evacuation data.
- ii. Reporting the influence of evacuation on crashes and finding the relationship between traffic state variables and crash risks.

- iii. Calibrating a microscopic traffic simulation model using real-world hurricane evacuation data, which can be utilized to understand driver behavior during evacuations, and
- iv. Providing experimental evidence of the potential safety impact of advanced driving assistance systems for transportation agencies during a hurricane evacuation.

We expect that this study will significantly contribute to the literature and practice of evacuation traffic safety by guiding us towards a proactive, crash-reducing evacuation management system.

## 2 Data Description and Exploration

In this project, we collected traffic and incident data from the Regional Integrated Transportation Information System (RITIS). This section presents a brief description of the data gathered and an exploratory analysis of it.

### 2.1 Data Description

We have collected the traffic data from RITIS (11), for I-75 northbound direction from September 3 to September 17, 2017, which includes the evacuation period of Hurricane Irma. To select the study location, we identified major evacuation routes in Florida and observed that a large portion of residents living in Florida evacuated to Georgia or adjacent states (12). Hence, we chose the segment between Wildwood and Gainesville (about 50 miles long), which served a major portion of the evacuation traffic during Irma. In addition, this segment of highway was equipped with detectors, such as microwave vehicle detection systems (MVDS), spaced approximately every 0.5 mile along the route. Each detector provides speed, volume, and occupancy data at a very high resolution (every 20 to 30 seconds).

We have also collected incident data for the study area from the RITIS incident database. The incident data covers four types of incidents: crash, weather-related incident, congestion, and other regular events (disabled vehicle, road construction delay, etc.) (Figure 2.1).

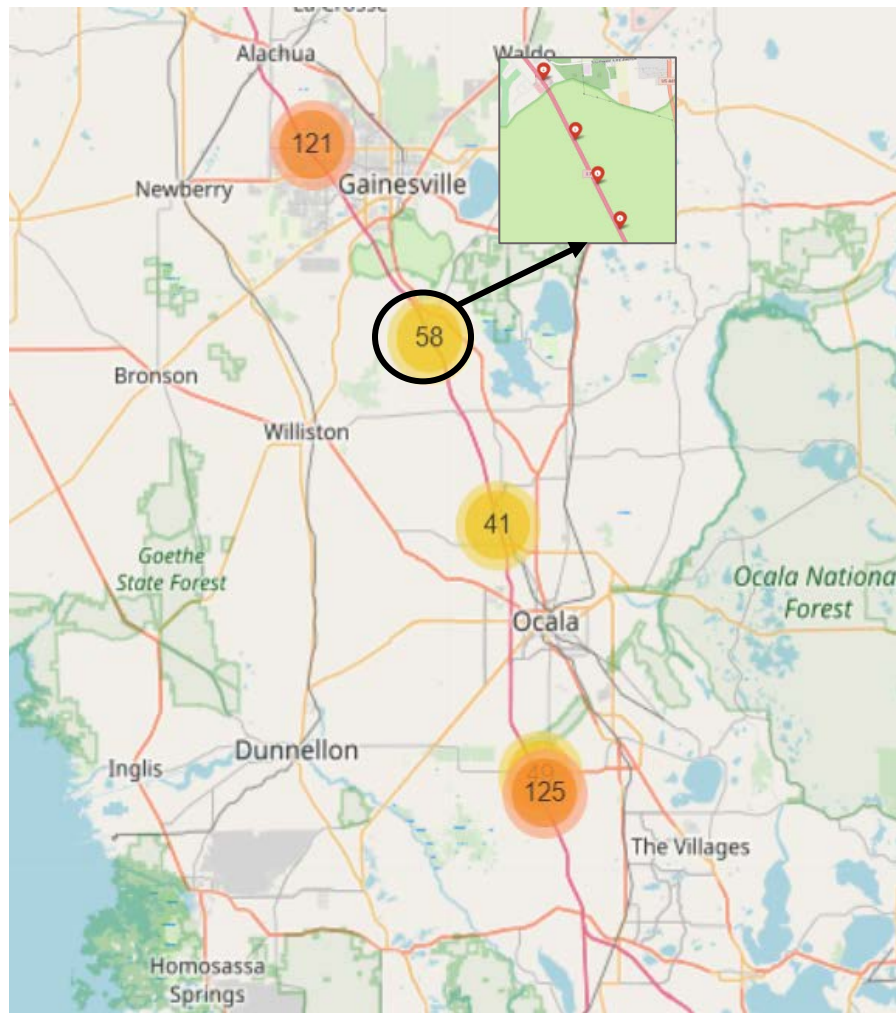


**Figure 2.1 - Crash locations aggregated in an Open Street map based on the actual coordinates of the crashes**

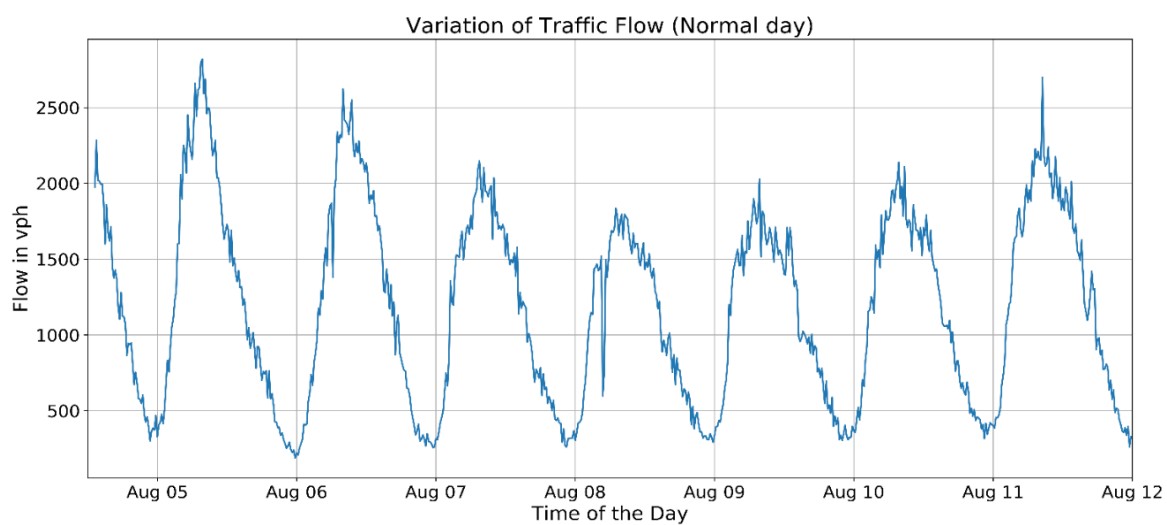
## 2.2 Data Exploration

In normal operating conditions, traffic flow shows predictable patterns such as heavy demand during peak hours, resulting in high traffic flows. Figure 2.2 (a) shows the distribution of traffic flow from August 5 to August 12, 2017, for the northbound traffic of I-75. A distinct morning peak in traffic congestion between 8 am and 10 am is observed. However, during an emergency event like a hurricane evacuation, overall traffic condition must bear severe disruption due to a drastic increase in traffic demand. Drastic oscillation and sudden flow breakdown are common characteristics of evacuation traffic. Figure 2.2 (b) shows the distribution of evacuation traffic from September 5 to September 9, 2017,

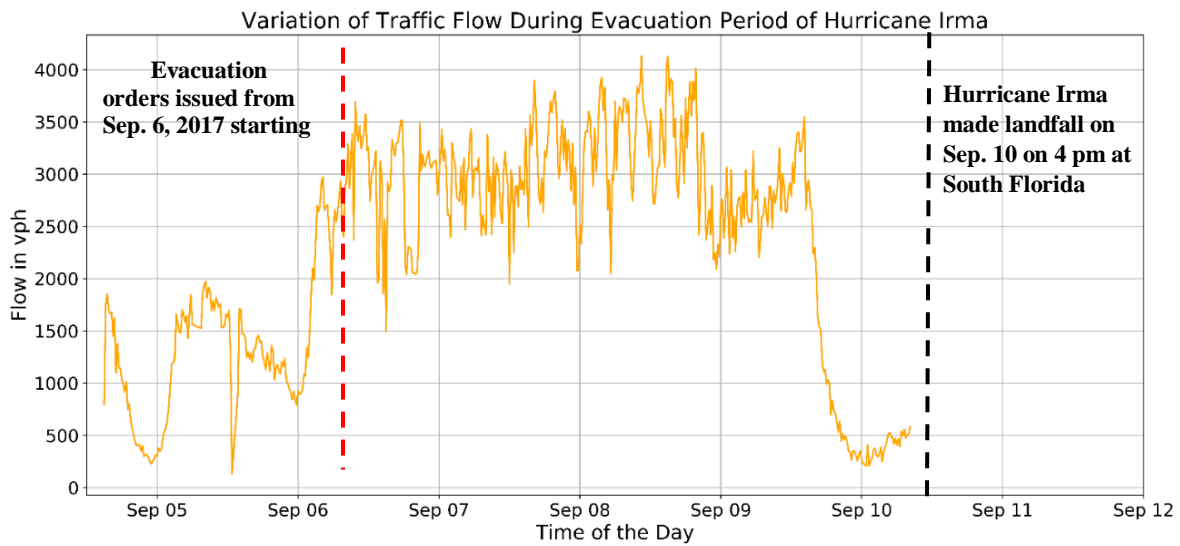
demonstrating traffic flow variation during the evacuation period of Hurricane Irma. We observe that during the evacuation period of Hurricane Irma, overall traffic flow is higher than a regular period, and shows irregular variations. Moreover, traffic conditions start to deteriorate just after the declaration of the evacuation order on September 6, 2017.

We could not extract any traffic data after September 9, 2017, and traffic flow variation cannot be shown after that time period. Hurricane Irma made landfall at the Florida Keys on September 10, 2017, as a category 4 storm. Irma then passed over several regions of Florida from September 10 to September 12, 2017, causing significant power outages in its path. Restoring the overall power system took about a week, and it is likely that the traffic detectors were malfunctioning, or the data collection server could not retrieve any information during that period.

Figure 2.3 shows the distribution of crashes on different dates during evacuation. An increase in the number of crashes from September 6 to September 8 can be observed, which include the evacuation period directly after the declaration of the state of emergency. The majority of the crashes during this period were rear-end collisions (about 51%).



(a)



(b)

Figure 2.2 - Traffic flow variation in regular and evacuation period

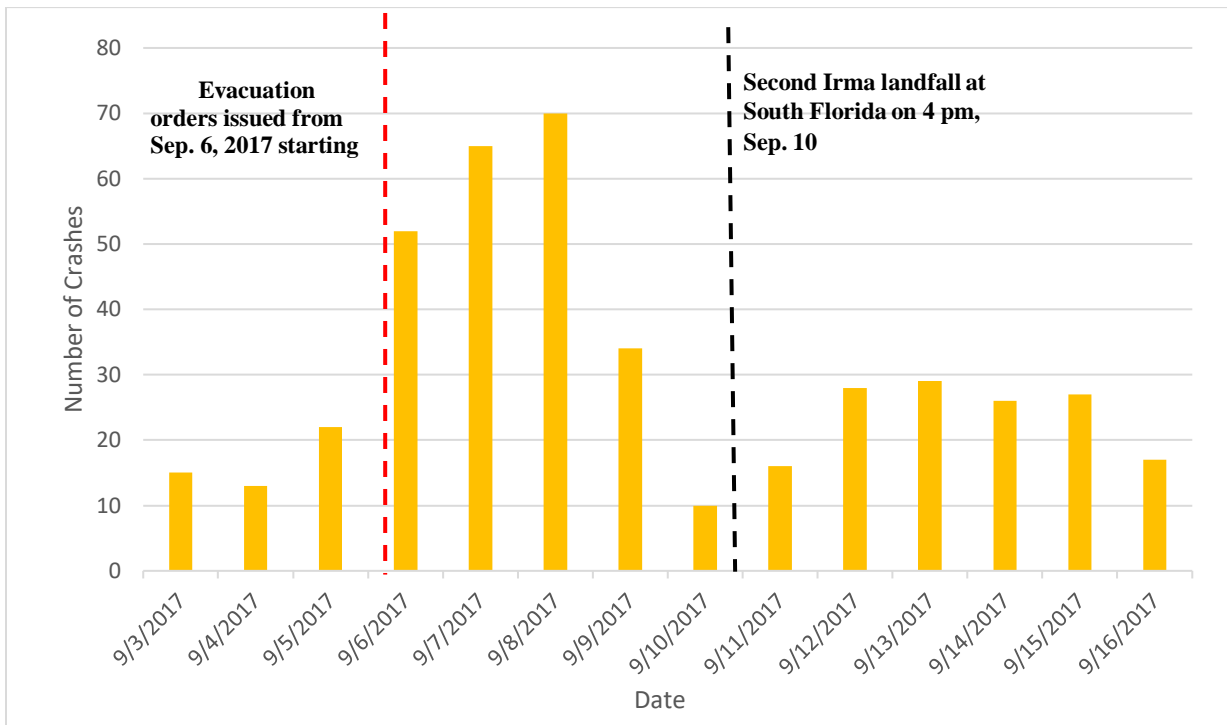
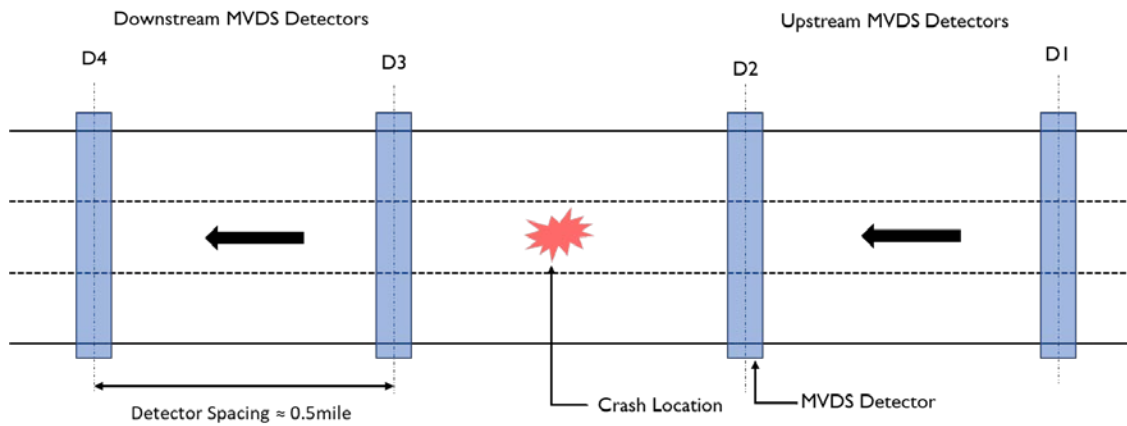


Figure 2.3 - Number of crashes during Hurricane Irma evacuation

### 3 Crash Risk Assessment During Evacuation

#### 3.1 Data Preparation

We mapped each crash event at its exact location and identify the two nearest upstream and downstream MVDS detectors (Figure 3.1). From these detectors, we extracted traffic speed, volume and occupancy data for a period of 30 minutes before the crash occurrence. For example, if a crash occurred on 2:00 pm, we extracted the data from 1:30 to 2:00 pm. A few detectors were not functioning during our study period, so we could not obtain traffic data from those detectors. Due to this lapse in data, we discarded the crashes corresponding to these detectors from our report. Finally, we created a dataset of 66 crashes during evacuation and extracted the traffic data from their corresponding upstream and downstream detectors from September 4 to September 9, 2017. To compare the traffic characteristics leading to a crash with non-crash traffic characteristics during the evacuation period, we also extracted the traffic data that corresponded to a non-crash condition for the same location on the same day. Since we are interested in understanding the influence of evacuation traffic on crashes, we do not have much flexibility to collect data for a non-crash condition on different dates/times during the evacuation period. However, during an evacuation period, there is no peaking pattern in traffic flow, so the time of the day or day of the week do not have any significant impact on traffic flow characteristics.



**Figure 3.1 - Layout of the segments and MVDS detectors**

When matching a non-crash data sample corresponding to each crash, we discard the traffic data that belongs to the 30 min period just before the crash occurrence and extract the data before that period. For example, if a crash occurred on 2:00 pm on August 5, 2017, we discard the data from 1:30 to 2:00 pm, and collect the data before 1:30 pm. We have also ensured that there is no overlap between two consecutive crash conditions in the case of multiple crashes. We assume that when a crash occurs it takes at least one hour for traffic to reach its normal operating condition, so if any data point fell within this time period, we discarded that as well. For example, if two crashes occurred at the same location on 2:00 pm and 5:00 pm on the same day, we extract the data from 3:00 pm to 4:30 pm as a non-crash condition. The 1 hr time period between 2:00 to 3:00 pm is considered as the time required for the traffic to reach normal operating condition, so we do not collect any data from this time period. We prepare the dataset so that each matched set (i.e., crash (1): non-crash ( $m$ )) belongs to the evacuation period within the same day. For each matched set, we are controlling for the day and location, matching non-crash traffic observations with a crash observation. In our final dataset, we have 63 crashes, which means 63 strata, each having 1 crash and  $m$  non-crash sample.

We have also collected crash data for non-evacuation periods at the same locations. In total, we obtained 78 crashes from August 1 to August 31, 2017, and for each of these crashes, we collected traffic data for 30 min periods before the crash occurrence. In this

case, a regular pattern in traffic flow variation (morning and evening peak, weekday, weekend, etc.) is observed. For matching the data related to a non-crash period with a crash data sample, we have accounted for the time-dependent variations of traffic characteristics. While preparing the data sample for non-crash case corresponding to each crash, we control the location, time of the day (e.g., 3:00 pm to 4:00 pm, 4:00 pm to 5:00 pm, etc.) and day of the week (e.g., Sunday, Monday, etc.). For example, if a crash occurred on Monday, August 5, 2017, at 3:50 pm at a particular location, we then search through the non-crash data for that location and select data corresponding to any Monday of that month, within a 3:00 to 4:00 pm time window. Like the previous case, we consider the pre-crash condition as the 30 min period before the crash occurrence, as well as control overlapping of multiple pre-crash conditions (i.e., 1 hr time period after the crash).

To extract the variables, we divided the sampled traffic data (20-30 sec resolution) into 5 min time intervals and aggregated them to estimate average speed ( $\bar{s}$ ), standard deviation of speed ( $ss$ ), coefficient of variation of speed ( $cvs = (ss/\bar{s})$ ), average volume ( $\bar{v}$ ) and average occupancy ( $\overline{oc}$ ) within that 5 min period. For each of the crashes, we have six time slices (1, 2, 3, 4, 5, 6), and each has five variables defining traffic states from four detectors (two upstream detectors and two downstream detectors). Though we have stated that the 30 min period before the crash occurrence is the pre-crash condition, several studies have shown that the traffic characteristics 5-10 min before the crash are the most significant when predicting real-time crashes (13, 14). We use the pre-crash condition as a 5 min time period ending at least 4 min before the crash occurrence. The time of the crash has been reported in the nearest 1 min, and the detector data has been aggregated for 5 min. If a crash occurred on September 6, 2017, at 4:39 p.m., then the corresponding pre-crash condition would be traffic data from 4:30 p.m. to 4:35 p.m. on that day.

To prepare the final dataset, we formed strata of crashes ( $N$ ); each stratum has one crash and corresponding  $m$  non-crashes. To form a stratum, we randomly selected the non-crash samples ( $m$ ) from the prepared matched non-crash dataset. Since we use five different ratios for crash to non-crash cases to form a stratum, we have five separate datasets for both evacuation and non-evacuation periods. Each dataset has  $N$  strata (number of crashes), and each stratum has one crash and corresponding  $m$  non-crashes (i.e.,  $m=1, 2, 3, 4, 5$ ).

### 3.2 Empirical Results

For each of the conditions (regular and evacuation), we have five separate datasets. Each dataset has  $N$  strata (depends on the number of crashes), and each stratum has one crash and corresponding  $m$  non-crashes. The number of non-crash samples varies from 1 to 5 (i.e.,  $m = 1, 2, 3, 4, 5$ ). For a matched sample and for each of the two upstream and two downstream detectors, we have four explanatory variables: 5 min aggregated mean values of occupancy ( $\overline{oc}$ ), volume ( $\overline{v}$ ), speed ( $\overline{s}$ ) and standard deviation of speed ( $ss$ ). Each dataset contains 16 variables in total. Previous studies (4, 15) found that the coefficient of variation of speed ( $cvs$ ) better captures the effects of speed and speed variation on crash risk. We combine the standard deviation of speed and mean speed to obtain  $cvs$ , which reduces the number of explanatory variables to three. Now, we have 12 variables associated with four detectors for each data set.

At first, we performed simple conditional logistic regression (only one variable at a time) for each of the variables. In total, we ran 12 models for each dataset. From the model results, we reported the hazard ratio for each variable. Hazard ratio is an estimate of an expected change in the risk ratio of having a crash against non-crash per unit change of a factor. This means that for a given exogenous variable, if the value of hazard ratio is greater than 1, the crash risk will increase with the increase of that variable. For each condition (regular and evacuation), we have five separate datasets and each dataset has

different sampling ratios (1:  $m$ ) between crash to non-crash cases. For each condition, we ran the models five times with five different datasets. However, each time, the model's estimates remained the same and the variables showed similar effects on crash risk. Therefore, we report the result only for one matching ratio (1:5). Table 3.1 presents the hazard ratio of all variables used in the analysis. We found that for a regular period, average occupancy and volume were not significant and the value of hazard ratio associated with these variables were close to one except for detector D1, which is located at the upstream of a crash location (see Figure 3.1). For detector D1, the value of hazard ratio associated with average occupancy (1.2334) is found to be significantly greater than 1. Similarly, for the evacuation period, average occupancy for each detector is significant, but the value of hazard ratio associated with these variables is not significantly greater than 1, except for detector D1 (1.1). The variables associated with detector D4 have been found insignificant for most cases, except for the average occupancy of evacuation data. However, the hazard ratio for this variable is close to 1, while upstream detector shows a larger value. In this analysis, we assessed the crash risk and our objective was to identify the factors which significantly increase crash risk. Therefore, we discarded all variables associated with detector D4.

**Table 3.1 - Hazard ratios for the matched sample (sampling ratio for crash and non-crash is 1:5)**

	Detectors	$\overline{oc}$	z	p-value	$\overline{v}$	z	p-value	<i>cvs</i>	z	p-value
Normal Period	D1	1.2334	1.194	0.232	1.0002	0.023	0.981	24.780	2.49	0.013
	D2	1.0648	0.364	0.716	0.9972	0.506	0.613	0.2267	0.985	0.324
	D3	0.9657	0.217	0.828	0.9946	0.993	0.321	13.231	1.882	0.0598
	D4	1.0277	0.157	0.875	0.9946	0.991	0.322	0.2958	0.855	0.392

Evacuation Period	D1	1.1	3.248	0.0247	1.0064	1.47	0.14	1.714	0.343	0.732
	D2	1.0455	2.245	0.0012	1.0027	1.045	0.296	2.489	0.629	0.529
	D3	1.0541	2.71	0.0067	1.0020	0.905	0.366	12.217	1.783	0.0745
	D4	1.0439	2.163	0.0305	1.0026	1.169	0.242	1.4886	0.866	0.387

We estimate the Pearson correlation coefficients between different pairs of variables show that volume is highly correlated with occupancy. In our final model, we use either occupancy or volume. Moreover, it appears that in some cases, the same variable (e.g., occupancy) over different detectors are also correlated with each other (Figure 3.2). For a given variable, we have decided to use its value observed in one detector instead of multiple detectors. We selected these variables based on the hazard ratio and corresponding significance probability ( $p$ -value).

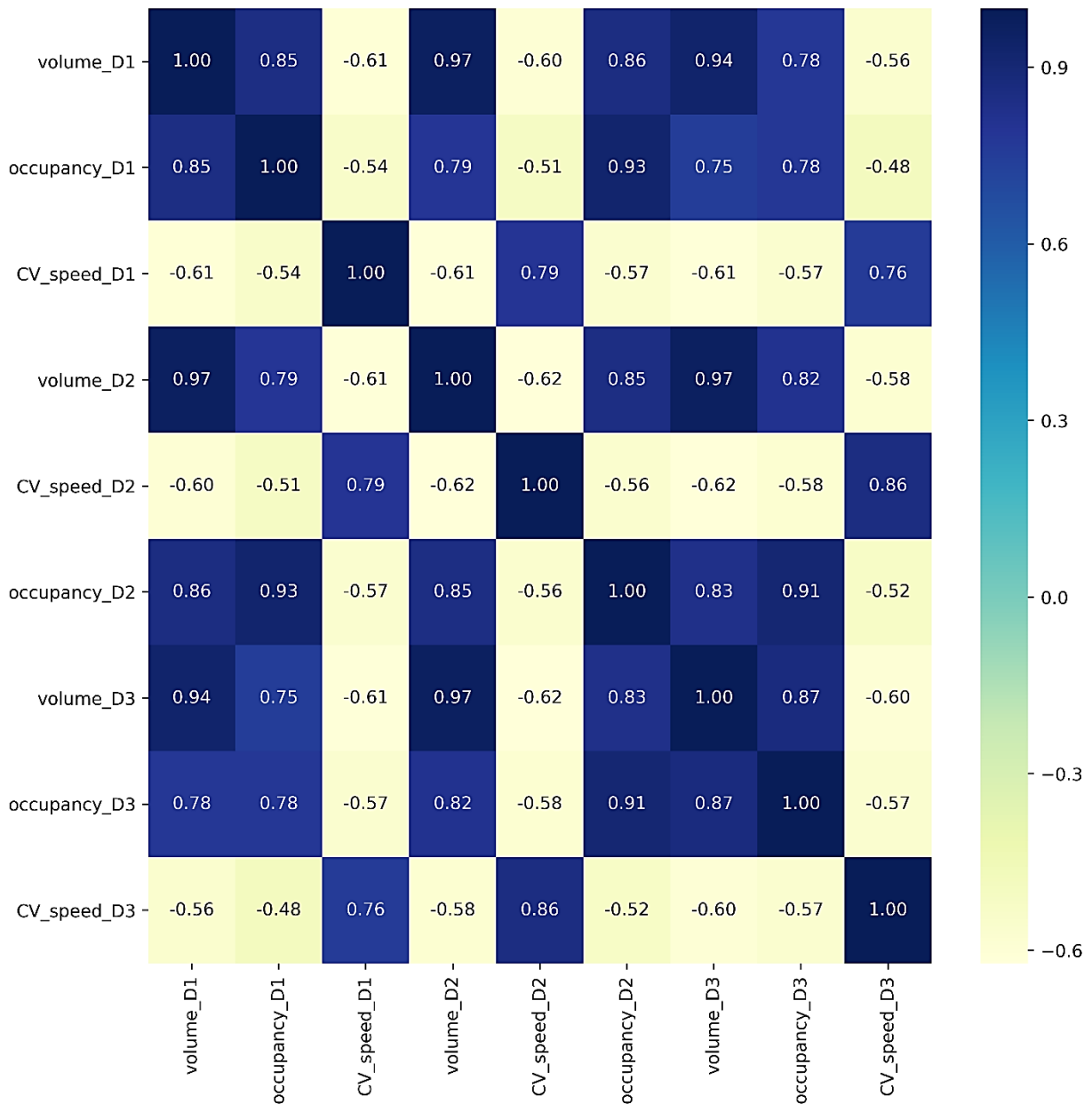


**Figure 3.2 - Pearson correlation values for different pairs of variables**

In our final analysis, we included different pairs of variables and ran the conditional logistic regression models for both evacuation and non-evacuation conditions. Table 3.2 presents the final results for each model. Under regular condition, the final models include two variables: mean occupancy and coefficient of variation of speed at D1. Both variables have a hazard ratio greater than 1, indicating that the odds of a crash increases with the increase of these variables. The mean occupancy variable associated with the upstream

detector D1 is significant at 95% confidence interval, while the other variable is significant at a 90% confidence interval. These estimates indicate if there is high occupancy of vehicles and large variation of speed at the upstream five to ten minutes before the crash, the chance of a crash occurrence increases. Since the coefficient of variation of speed includes the average speed as the denominator, this also indicates that the average speed is lower in crash cases.

Under an evacuation condition, the final models have two significant variables: coefficient of variation of speed for the downstream detector D3 and mean volume for the upstream detector D1. The value of hazard ratio for both variables is greater than 1, which means that if there is a high volume of traffic at upstream and high variation of speed at downstream, then the chances of crash occurrence is higher. We can interpret the combined effects of these variables increase the likelihood of crash occurrence, at a location in between these two zones (upstream location and downstream location). Detector D1 at the upstream zone and detector D3 at the downstream zone are placed 1 mi apart, so during the evacuation period this one-mile segment experienced high-speed variation, high volume of traffic, and lower average speed, which indicates potential queue formation under oscillatory speed conditions. Consequently, this would have caused a significant increase in number of crashes within this segment.

**Table 3.2 - Hazard ratio for the final models for evacuation and regular period  
(sampling ratio for crash and non-crash is 1:5)**

	Variables	Conditional Logistic Regression		
		Hazard Ratio	<i>z</i>	<i>p</i> -value
Regular Period	cvs_D1	40.083	2.76	0.0059
	Occupancy_D1	1.367	1.74	0.0830
Evacuation Period	cvs_D3	17.55	2.068	0.0386
	Volume_D1	1.004	1.786	0.0741

In a matched case control study, we control the confounding variables to estimate a conditional logistic regression model. By doing so, we lose the power to estimate individual group effect (e.g., effect of matching variables) on crash risk. For instance, if we want to estimate whether the event evacuation itself has any influence on crash risk, we cannot estimate that using a conditional logistic regression model. Because of this, we also perform unconditional logistic regression with the unbalanced data, including all data samples rather than matched samples. In this model, we implemented combined data, both evacuation and non-evacuation data, and added a dummy indicator variable “*Ev*” (0 or 1) to indicate the evacuation related data samples and non-evacuation related data samples.

Table 3.3 presents the estimates from an unconditional logistic regression model. We found the results to be similar to the conditional logistic regression estimated over the matched data set. The estimates associated with coefficient of variation of speed for detector D3 and the mean volume for detector D1 are significant. The variable *Ev* is also

significant, indicating that during evacuation the likelihood of crash occurrence increases, compared to the regular period.

**Table 3.3 – Coefficient estimates for unconditional logistic regression**

Variables	Coef.	Std.Err.	z	p-value
volume_D1	0.0049	0.001	4.8141	<0.0001
cvs_D3	0.8459	0.2344	3.6083	0.0003
Evc	0.8397	0.2051	4.0946	<0.0001
Constant	-9.4934	0.2005	-47.3375	<0.0001
Pseudo R-squared	0.032			
AIC	2496.141			
BIC	2541.111			
No. of Observations	563748			
Log-Likelihood	-1244.1			
LL-Null	-1285.5			

### 3.3 Summary

Our investigation reveals traffic flow characteristics during hurricane evacuation using real-world data from Hurricane Irma's evacuation period. As expected, it shows that during evacuation overall traffic demand is higher than the regular traffic condition, causing irregular variation of traffic flow. Consequently, it leads to significant variations of traffic speed, resulting into a stop-and-go traffic situation. Previous studies found that traffic speed variation is one of the contributing factors for an increase in the number of crashes.

Adopting a case-control study approach, we find that during evacuation, the coefficient of variation of speed at the downstream station and average occupancy at the upstream station of a crash location significantly affect crash likelihood. This implies that higher

occupancy rates at upstream, coupled with high variation in speed at downstream locations, increase the likelihood of crash occurrence. Moreover, an unconditional logistic regression model applied over combined (including both evacuation and non-evacuation period) data showed that evacuation itself increases the chance of a crash occurrence, even after we account for traffic characteristics.

#### **4 Microscopic Simulation of Evacuation Traffic**

In this section, we assessed the safety impacts of an ACC system during an evacuation period. ACC systems are commonly designed to maintain a constant time-gap (CTG) between vehicles when following a vehicle. Several studies have shown that the ACC system substantially reduces traffic collisions, especially rear-end crashes, under regular traffic conditions. We developed and calibrated a microscopic traffic simulation model, known as SUMO, to replicate the evacuation traffic behavior. We then added ACC-equipped vehicles at different market penetration rates (MPR) to monitor the overall improvement in traffic collisions.

##### **4.1 Data Preparation**

We have selected a 9.5 mi segment on I-75 between Ocala and Gainesville, Florida: a road segment which serves a major portion of the evacuation traffic during Irma. For this location, we extracted the data from 11 MVDS detectors (Figure 4.1 (b)). Among these detectors we were unable to extract any data from three detectors. These detectors may have been dysfunctional during that period, unable to receive traffic information. Each MVDS detector provides speed, volume, and occupancy at a high resolution (every 20-30 sec).

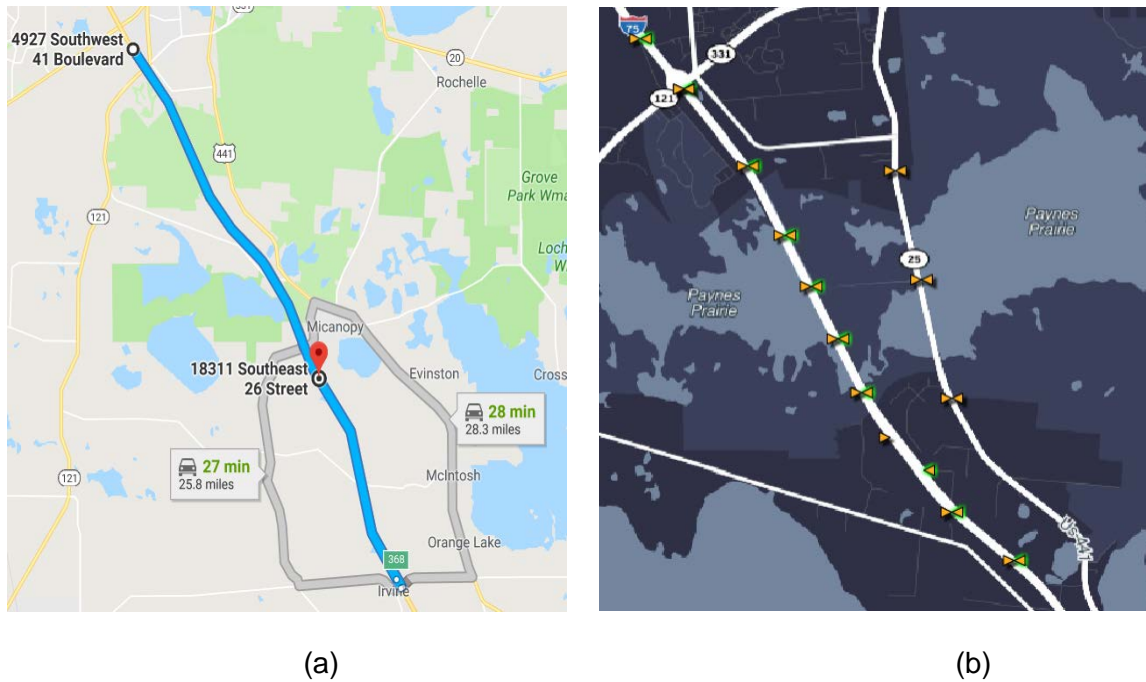


**Figure 4.1 - Study segment on I-75: (a) Google Map view of the route (b) Location of the MVDS detectors**

For each data set, we aggregated traffic volume and speed for 5 min intervals, and for each interval, we calculated the average flow (Figure. 4.1(b)) and average speed. While processing the data, we observed some were missing values for speed and volume. We applied a simple rolling average method with a window size of 3 to replace the missing values (by taking the average from previous three available interval values). We also checked if there were any outliers in our dataset. We used 1.5 times the interquartile range (IQR) as the boundary. The IQR is the difference between the first quartile ( $Q_1$ ) and the third quartile ( $Q_3$ ) of a data sample. Outliers are defined as observations that fall below  $Q_1 - 1.5 IQR$  or above  $Q_3 + 1.5 IQR$ . From this process, we observed very few outliers. Similar to missing values, we replaced the outliers using the rolling average method.

We also collected incident data for the study area from the RITIS incident database. The incident data covers four types of incidents: crash, weather-related incident, congestion, and other regular events (disabled vehicle, road construction delay, etc.).

#### 4.2 Car-Following Model in SUMO

In this study, we developed a micro-simulation model of evacuation traffic in SUMO (16) version 1.2.0. We used the Krauss collision-free model (17), which is the default car-following model for SUMO. Though the Intelligent Driver Model (IDM) has been widely used for car-following modeling, studies have shown that the IDM provides greater errors in speed than the Krauss model in unsteady traffic conditions. This is especially evident for cars and heavy vehicles (18) because IDM does not perceptibly follow the speed changes of the preceding vehicle (19) in an unsteady state. The Krauss model is a microscopic, space continuous car-following model, which is essentially a stochastic version of the Gipps model (20). The model was developed by Krauss in 1997, based on the concept of safe speed, where the safe speed is computed as follows:

$$v_{safe} = v_t(t) + \frac{g(t) - v_n(t)t_r}{\frac{v_n(t) + v_{n-1}(t)}{2b_m} + t_r} \quad (1)$$

where  $v_n(t)$  and  $v_{n-1}(t)$  represent the speeds of the leading and following vehicles at time  $t$ ,  $g(t)$  is the gap to the leading vehicle at time  $t$ ,  $t_r$  is the driver's reaction time (about 1 sec) and  $b_m$  is the maximum deceleration of the vehicle ( $m/s^2$ ). In a car-following scenario,  $v_{safe}$  can be larger than the maximum speed ( $v_{max}$ ) allowed on the road or larger than the vehicle's physical acceleration capabilities. To prevent this, the desired speed of the vehicles is calculated. The desired speed ( $v_{des}$ ) of each vehicle is the minimum of the safe speed  $v_{safe}$ , the current speed plus the maximum acceleration and the maximum speed [20]:

$$v_{des(t)} = \min[v_{safe}(t), v(t) + at, v_{max}] \quad (2)$$

To account for human-error-related imperfection for human drivers, a random error was subtracted from the desired speed

$$v(t) = \max[0, \text{rand}[v_{des}(t) - \epsilon_a, v_d]] \quad (3)$$

We used the Krauss model to simulate human-driven vehicles in SUMO. The default parameters for the model can be found in the literature (21). To select the base model, we reviewed several studies, though all the studies were done for regular traffic conditions. We used these parameter values in our initial model. Through the calibration process, we changed these parameters to represent the evacuation condition. The parameters for the initial model are given in Table 4.1. Here, the parameter sigma has been introduced to model a driver's imperfection to adapt the speed of a traffic stream. If the value of sigma is above 0, drivers with the default car-following model will drive slower than the possible safe speed; the value will be chosen from a random distribution between [0, acceleration]. Tau indicates the reaction time for the drivers, which varies from 1.0 to 1.5 sec.

**Table 4.1 - Initial model before adjusting the parameters**

Vehicle Types	Max Sped (m/s)	Speed Factor norm (mean, deviation, min, max)	Min Gap (m)	Car Following Model	Max Accel (m/s <sup>2</sup> )	Max Decel (m/s <sup>2</sup> )	Sigma	Tau (s)
Car	70	normc(1,0.1,0.2,2.0)	3.0	Krauss	3.0	5.5	0.5	1.0
HGV	65	normc(1,0.1,0.2,2.0)	3.0		3.0	5.5	0.5	1.0

In a traffic stream, the desired driving speed usually varies for different vehicles. This can be modeled by defining the attribute "speed factor," which allows a vehicle to draw "speed factor" from a normal distribution. This parameter can be given as "norm (mean, dev)" or "normc (mean, dev, min, max)". For instance, if we choose the speed factor as "normc (1, 0.1, 0.2, 2)", then it will result in a speed distribution where 95% of the vehicles drive between 80% and 120% of the legal speed limit.

To simulate the car-following behavior for an ACC vehicle, we use the ACC model developed in the literature (19–23). The detail implementation and default parameter

settings of the model can be found in the literature (24). The ACC model consists of four control algorithms: cruising (or speed) control, gap-closing control, gap control, and collision avoidance mode. For each of the four models, we use the calibrated parameter setting as stated in the literature (19–23), which is provided in Table 2. Each of the parameters controls the acceleration of the following vehicle based on the speed and gap difference with the preceding vehicle. Moreover, if there is no preceding vehicle within the range of the sensor or if preceding vehicles exist in a spacing larger than 120 m, then only control mode will operate, and the vehicle will maintain the speed pre-defined by the driver (driver's desired speed).

**Table 4.2 - Controller parameters for ACC**

Parameters	Value	Remarks
Speed Control Gain	$0.4 \text{ s}^{-1}$	Cruising Model
Gap Control Gain Space	$0.23 \text{ s}^{-2}$	Car following Model
Gap Control Gain Speed	$0.07 \text{ s}^{-1}$	Car following Model
Gap Closing Control Gain Space	$0.04 \text{ s}^{-2}$	Approaching Model
Gap Closing Control Gain Speed	$0.80 \text{ s}^{-1}$	Approaching Model
Collision Avoidance Gain Space	$0.8 \text{ s}^{-2}$	Collision Avoidance Model
Collision Avoidance Gain Speed	$0.23 \text{ s}^{-1}$	Collision Avoidance Model

#### 4.3 SUMO Simulation Model Development and Calibration

To design simulation experiments in SUMO, we would need a well-calibrated model. This requires representing the real-world network in the simulation environment with proper geometric features. To replicate the real-world scenario, we imported the traffic network for I-75 from the Open Street map and converted this network into a SUMO network file. We simulated a 9.5 mi segment between Ocala and Gainesville that includes

two entry and exit ramps. We adjusted the traffic network using SUMO network editor and removed all unnecessary routes and nodes.

In the simulation, we included two types of vehicles: passenger car (PC) and heavy goods vehicle (HGV). We do not have the exact distribution of PC and HGV for that study period. However, in most cases, the HGV percentages varied from 2 to 5% of the total number of vehicles. For our simulation, we assumed the HGVs as 4%, which was adjusted during the calibration process. We obtained the traffic volume from RITIS database at 20-30 sec resolution, aggregated them into 5 min intervals, and converted this volume into a 5 min average flow. Because we are simulating a 2 hr period, we input the average interval flow for a 2 hr period. From the analysis, we found that the maximum number of crashes occurred on September 8, 2017, between 2:00 pm and 5:00 pm (Figure 2.3). Therefore, we chose the time window of 1:30 to 3:30 pm for our simulation experiments. After excluding the first 30 min of simulation warm-up time and the last 30 min of cool-down time (no statistics were collected during this time), 60 min of simulation data (2:00 to 3:00 pm) were used for calibration and validation.

For calibrating the model, we added eight loop detectors on the network at the exact location of the MVDS detectors (see Figure 4.1). From the loop detectors, we obtained aggregated volume and average speed for 5 min intervals. We use Geoffrey E. Heaver (GEH) statistics (25) and modified chi-square statistics to compare the filed volume with the simulation. GEH statistics incorporate both relative and absolute differences between the two groups. The GEH can be stated as follows:

$$GEH = \sqrt{\frac{2 * (M_{obs}(n) - M_{sim}(n))^2}{(M_{obs}(n) + M_{sim}(n))}} \quad (4)$$

We calculate the GEH for each detector (i.e. 8 detectors) and each time interval (i.e. 2:00 pm to 3:00 pm, 12 total intervals). We also estimated the root mean square error (RMSE) and root mean square percentage error (RMSPE). To check the compatibility of

the developed model, we reviewed several specifications. However, all of the specifications for calibrating a traffic simulation model are given for regular traffic conditions. For an evacuation period, traffic variation is significantly higher than a regular period and it is difficult to achieve more accurate data. Because of this, there should be an alternative set of guidelines for calibrating models for an evacuation period. We still followed the standards mentioned by Nezamuddin et al. (26), which recommended for 85% of the data point, the GEH value should be less than 5 and the absolute speed difference (ASD) between simulated speeds and field speeds should be within 5 mph (or 2.5 m/s). Our objective is to keep the GEH less than 5 and absolute speed difference below 2.5 m/s.

First, we selected the speed distribution of vehicles based on the field measurement. The measurement was slightly adjusted during the calibration process. We then changed each parameter within a certain range, which was selected based on previous studies and engineering judgment (Table 4.3).

**Table 4.3 - Parameter setting for model calibration**

Types	Proportion	Min Gap (m)	Max Accel. (m/s <sup>2</sup> )	Max Decel. (m/s <sup>2</sup> )	Sigma	Tau (s)
Car	94% to 98%	2.0 to 3.0	3.0 to 4.5	5.0 to 7.5	0.1 to 0.5	1.0 to 1.5
HGV	2% to 4%	2.0 to 3.0	3.0 to 4.5	5.0 to 6.5	0.1 to 0.5	1.0 to 1.5

We ran the simulation several times with different sets of parameters, and each time we checked the GEH, ASD, RMSE and RMSPE values. Due to the large variation of speed

and flow, it was challenging to achieve more accurate levels for simulating evacuation traffic. We presented the final parameters for the model in Table 4. We ran the final model 20 times with random seeds, and each time we estimated the GEH, ASD, RMSE, and RMSPE. Finally, we estimated the average value for each of these metrics (Table 5). About 73% of the observations show a GEH value less than 5, at the same time 73.22% of the observations show ASD value below 2.5 m/s. RMSE for speed is less than 5m/s, which indicated that the model is reasonably calibrated to capture the speed variations occurring during an evacuation period. As shown in Figure 2.2, there was some drastic change in traffic speed at certain points which induced a large error in our model (high absolute difference). We were unable to capture this variation with the simulation model. Evacuation traffic modeling is a challenging task which requires different standards and specifications to check the performance of the calibrated model. Currently, such standards do not exist for evacuation traffic models.

In our final model, values of maximum acceleration and deceleration were higher than the regular car-following model (see Table 4.1) for normal traffic condition. This indicates that abrupt changes in speeds and a higher rate of acceleration are typically followed in evacuation. In a stop-and-go traffic condition, drivers are more likely to take every opportunity to accelerate to recover the delays induced by a repetitive breakdown in traffic flow. Also, the value for the minimum gap parameter was 2.0 m. For the regular condition, the value for the minimum gap parameter varied from 2.5 to 4 m. This is plausible because in a highly congested condition, evacuation drivers are more likely to reduce the gap with the leader. Also, drivers attempt to maintain a minimum time gap of  $\tau$  between the rear bumper of their leader and their own front-bumper. In our case, the value of  $\tau$  is 1.2, which is less than the usual reaction time of 1.5 seconds under a regular traffic condition. These changes in parameters from a regular traffic condition indicate potential crash risks during an evacuation period.

**Table 4.4 - The final model after adjusting the parameters**

Types	Proportion	Max Speed (m/s)	Speed Factor norm (mean, deviation, min, max)	Min Gap(m)	Car Following Model	Max Accel. (m/s <sup>2</sup> )	max Decel. (m/s <sup>2</sup> )	Sigma	Tau (s)
PC	98%	70	normc(0.96,0.3,0.2, 1)	2.0	Krauss	4.5	6.5	0.2	1.2
HGV	2%	65	normc(0.96,0.3,0.2, 1)	2.0		4.5	6.5	0.2	1.2

**Table 4.5 - Values of the performance metrics for the calibrated model**

Metrics	Average values for Flow	Metrics	Average values for Speed
GEH <5	72.91 % of the total observations	ASD <2.5 m/s	73.22% of the total observations
RMSE	278.863	RMSE	4.738
RMSPE	12.312	RMSPE	20.76

#### 4.4 Surrogate Safety Measures

A simulated environment does not explicitly show the collisions between two interacting vehicles. Hence, we needed some surrogate measures to represent interactions between vehicles in a traffic stream and to identify potentially unsafe conditions. To evaluate crash risks from simulation models, previous studies have used several surrogate safety measures such as time to collision (TTC), post encroachment time (PET), rear-end crash risk index, deceleration rate to avoid a collision (DRAC). In this

study, we used one temporal proximity-based indicator (TTC) and one deceleration-based indicator (DRAC) to evaluate the impact of ACC-equipped vehicles on crash risks.

The TTC measure, first introduced by Hayward (27), is defined as the expected time for two vehicles to reach a common position on the road, given that their speed and trajectory remain the same. If the following vehicle  $n$  moves faster than the preceding vehicle ( $n-1$ ), then TTC can be evaluated by using Equation 5.

$$TTC_{n(t)} = \begin{cases} \frac{x_{n-1}(t) - x_n(t) - L_{n-1}}{v_n(t) - v_{n-1}(t)}, & \text{if } v_n(t) > v_{n-1}(t) \\ \infty, & \text{if } v_n(t) < v_{n-1}(t) \end{cases} \quad (5)$$

where  $TTC_{n(t)}$  denotes the TTC value of the vehicle  $n$  at time  $t$  and  $x, v, L$  denote the position, speed, and length of the corresponding leading ( $n-1$ ) and following ( $n$ ) vehicles, respectively. Researchers have used different threshold values (1.0, 1.5, 2.0, etc.) of TTC to identify whether two vehicles will collide or not (7, 28–33). Van der Horst and Hogema (34) suggested that the preceding vehicle and following vehicle are assumed to be in a collision if the TTC value for the following vehicle is less than 1.5.

In an oscillatory traffic condition (stop and go traffic), deceleration-based indicators are more critical. We used the deceleration rate to avoid a collision (DRAC) to consider the effect of speed differentials and decelerations on crash risks. DRAC, first introduced by Cooper and Ferguson (35), indicates the maximum deceleration rate needed to be applied by a vehicle to avoid a collision with another vehicle. In the case of a car following scenario, the preceding vehicle ( $n-1$ ) is responsible for initiating action such as braking, lane changing, etc. while the following vehicle ( $n$ ) must react to this action by braking. For this rear-end interaction, the DRAC for the following vehicle  $n$  can be expressed as follows:

$$DRAC_n^{REAR} = \frac{(v_n(t) - v_{n-1}(t))^2}{2[(x_{n-1}(t) - x_n(t))]} \quad (6)$$

where  $v, x$  denote the speed and position of the corresponding leading ( $n-1$ ) and following ( $n$ ) vehicles, respectively. Several studies have recognized the relevance of DRAC to measure crash risk and crash severity. They have also introduced different

severity levels based on a different range of DRAC values. The American Association of State Highway and Transportation Officials (AASHTO) (36) recommends that the maximum comfortable deceleration rate for most of the drivers is  $3.4 \text{ m/s}^2$ . Archer (37) suggested that if, for a given vehicle interacting with a preceding vehicle, the DRAC value is greater than  $3.35 \text{ m/s}^2$ , the vehicle is assumed to be in a collision with the preceding vehicle. In this study, we use the threshold values for TTC as 1.5 sec and for DRAC as  $3.30 \text{ m/s}^2$ .

#### 4.5 Simulation Results

To estimate the surrogate safety assessment measures, we equipped the vehicles with SSM (surrogate safety measures) devices (38). Each SSM device provides an estimate of TTC and deceleration rate to avoid a collision (DRAC) value for the study corridor. Based on previous studies, we chose threshold values for TTC and DRAC as 1.5 sec and  $3.30 \text{ m/s}^2$ , respectively, to identify the number of conflicts that can lead to potential traffic collisions. This means that if TTC and DRAC value between the leading and preceding vehicle is less than the threshold value of TTC and greater than the threshold value of DRAC, we identified it as a potential collision.

We ran the final model 10 times with random seeds to eliminate any random effects. For each simulation run, we estimated the number of potential collisions and reported the average value, aggregating all results for different simulation runs. From simulation results, we found that the average number of conflicts leading to potential collisions for the base condition is 264. We follow the same procedure to estimate the number of potential collisions for different levels of market penetration of ACC-equipped vehicles.

In an ACC system, the controlling parameters allow a vehicle to maintain a constant gap with the preceding vehicle. By fixing the desired headway, the ACC-equipped vehicle can maintain a safe cruising distance. Furthermore, the reaction time for the ACC-equipped vehicle (0.1 sec) is less than a manually driven vehicle. Consequently, desired

time headway (1.1 to 1.6 sec) is also less than a manually driven vehicle (1.5 sec)(39). In this experiment, we chose four levels of market penetration of ACC-equipped vehicles and used four values of desired time headway. At a given market penetration, we ran the simulation with four different values of desired time headway, and for each case, we estimated the TTC and DRAC values. The experiment result shows that if we fix the desired time headway greater than 1.2 sec, the number of potential collisions decrease with the increase in the penetration rate of ACC-equipped vehicle (see Figure 4.2). When the desired time headway is 1.2 sec, the result showed some discrepancies. For instance, the number of conflicts leading to potential collisions decreased with the increase in MPR of ACC-equipped vehicles up to 50%, but after that, it increases with the increase of ACC-equipped vehicles. Nevertheless, the number of potential collisions always remains less than the base condition.

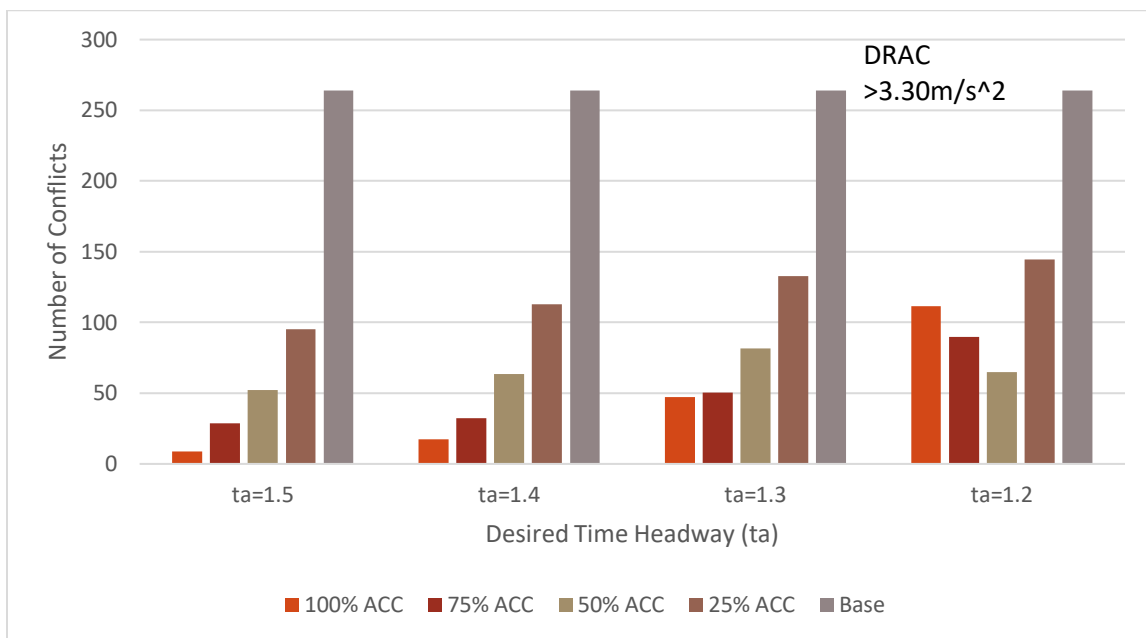


**Figure 4.2 - Variation of number of conflicts for different values of desired time headway**

We performed two-sample t-tests to measure the difference between the base condition with the other scenarios and estimated the significance of this differences ( $p$ -value). In Table 6, we included the t-test results for ACC-equipped vehicles with the

desired headway of 1.3 sec. From the result, we observe that with only a 25% market penetration rate of ACC vehicles, we can achieve about 49% of reduction in the number of conflicts. Further improvement in traffic conflicts can be achieved at 75% market penetration rates of ACC-equipped vehicles. Reduction in the number of conflicts is almost same (around 80%) for both 75% and 100% MPR. We also conducted the same analysis with different values of desired headway and for each case, we saw similar outcomes.

**Table 4.6 - Percentage change in the number of conflicts averaged over 10 simulation runs (desired time headway is 1.3 sec)**

	Estimate	Value	Mean Difference	% change in mean value	p-value	upper bound	lower bound
Base (no ACC)	mean	264	N/A	N/A	N/A	N/A	N/A
	standard deviation	51.29					
Base + 25% ACC	mean	100.2	131.4	49.77%	<0.0001	119.53	208.06
	standard deviation	42.53					
Base + 50% ACC	mean	81.6	182.4	69%	<0.0001	147.34	217.459
	standard deviation	12.39					
Base + 75% ACC	mean	50.2	213.80	80.98%	<0.0001	179.12	248.47
	std standard deviation	9.64					
100% ACC	mean	47.4	216.60	81.82%	<0.0001	181.43	251.76
	standard deviation	13.06					

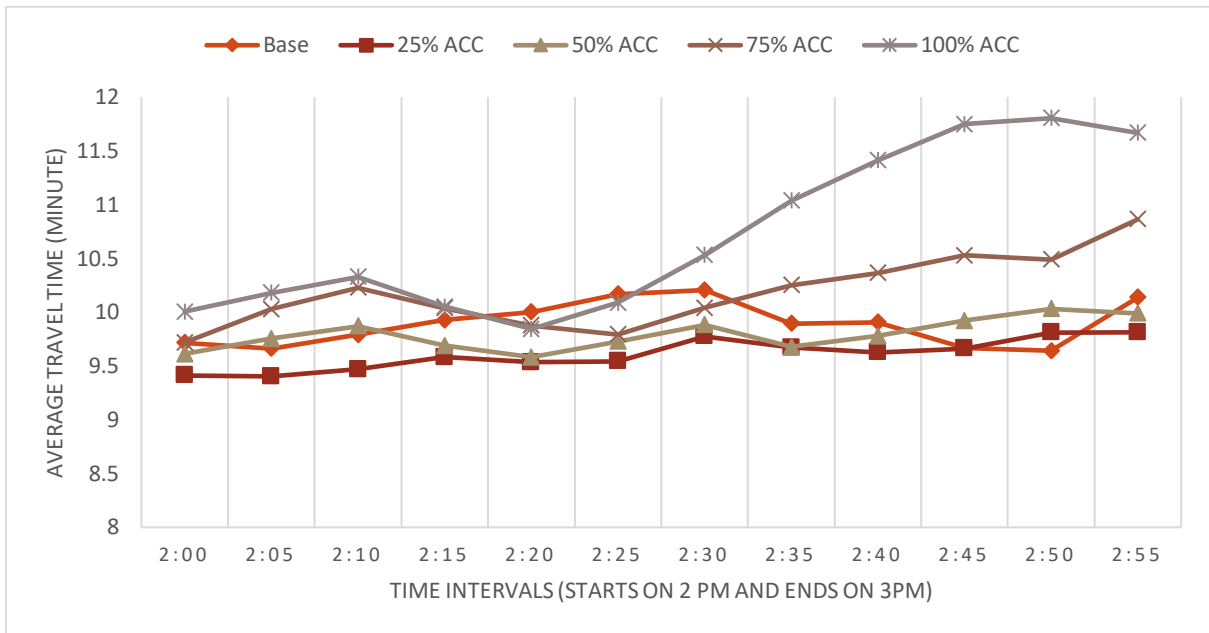


**Figure 4.3 -Travel time variation at different market penetration rate of ACC vehicles**

We also collected the average travel time for the base scenario, as well as for different MPR of ACC-equipped vehicles. We have observed that with the increase in the percentage of ACC-equipped vehicles, average travel time reduces from the base condition. However, for 75% or 100% MPR of ACC, the travel time increases. The average travel time for the base condition is 9.7 min, whereas at 100% MPR of ACC-equipped vehicles, average travel time is 10.8 min. This variation can be attributed to the fact that the ACC system decreases the sudden changes in the rate of acceleration, which reduces sharp changes in traffic speed. Consequently, the overall speed reduces to adapt to the traffic stream.

#### 4.6 Summary

In this section, we developed and calibrated a microscopic traffic simulation model to analyze driving behavior during evacuation. The model was calibrated using real-world evacuation traffic data collected during Hurricane Irma. For the calibrated model, the values of maximum acceleration and deceleration were found to be  $4.5 \text{ m/s}^2$  and  $6.5 \frac{\text{m}}{\text{s}^2}$ ,

respectively. These values are greater than those in typical car-following models calibrated under regular traffic conditions. Also, larger acceleration and deceleration values indicate abrupt speed variation, which is the most common scenario for evacuation traffic.

Using the calibrated micro-simulation model, we evaluated the safety impacts of ACC-equipped vehicles on crash risks. Adopting two surrogate safety measures, TTC and DRAC, we have found that ACC-equipped vehicles can significantly reduce the number of potential collisions during evacuation. The results also indicated that the safety impact of the ACC system largely depends on its parameter settings of ACC controllers. By fixing the desired time headway at a value greater than 1.2 sec, the number of potential collisions can be reduced by 49.7%. At the same time, we have also found that if we keep the MPR of ACC vehicles below 50%, average travel time improves over the base condition. This is a promising result considering that an MPR of 25% to 50% of ACC vehicles is more likely in the future than 75% to 100% MPR of ACC vehicles.

This study has several limitations. Our findings rely on simulation experiments that do not fully mimic real-world evacuation traffic conditions. We calibrated the simulation model with real evacuation traffic data, which shows a disperse distribution for speed. It is challenging to select an accurate distribution of speed to match the speed variation of the simulated vehicles with real-world data. To check the performance of our model, we used GEH statistics and absolute speed difference. Recommended values for these metrics are conservative and are suitable only for normal traffic conditions. Therefore, we believe that new guidelines should be developed to calibrate traffic simulation models for evacuation traffic scenarios.

## 5 Implications of the Research

This study has several implications, as follows:

- The outcome of the study can be utilized to develop a crash prediction model that will work for both regular and evacuation traffic. Consequently, proactive measures can be developed to reduce crash occurrence during an emergency situation. Particularly, this method will help identify potential crash locations created by prevailing traffic conditions during an evacuation. This can be used to warn evacuee drivers about the impending crash risk and enforce them to reduce travel speed to a certain limit.
- The study has further implications for evacuation declarations. Our result shows that high volume and occupancy of traffic during evacuation are key contributing factors for accidents. If the volume of traffic on evacuation routes can be reduced, the chances of crash occurrence will significantly decrease. However, during evacuation, traffic demand surges directly after an evacuation order is declared due to the large number of people entering a roadway at the same time from different zones. One potential strategy should be phased declaration of evacuation orders, which require identification of primary risk zones based on spatial and temporal information on hurricane landfall. Evacuation orders should be declared in a phased manner starting with the primary risk zone and then other zones based on potential hurricane threat.
- The study also found that typical parameters of car-following models should be adjusted to account for an evacuation condition. Researchers and practitioners should consider our findings when using micro-simulation tools for modeling evacuation traffic.
- This study evaluates the safety impact of different driving assistance systems on crash occurrence during evacuation. The findings are promising as it has

been shown that the ACC system could potentially reduce the number of crashes during evacuation. It is worth noting that most modern cars are equipped with an ACC system. However, the lack of public knowledge on how to use them, as well as the high level of mistrust in such emerging technology, discourages drivers from using this type of vehicle driving assistance technology. Transportation and emergency management agencies should take necessary steps to acquaint drivers with new in-vehicle technologies and their potential benefits in an emergency situation such as hurricane evacuation.

This study opens several new avenues for future research. For instance, future work should assess the safety and mobility impact of connected vehicles with platooning and cooperative adaptive cruise control systems. Studies should also investigate the impact of vehicle to vehicle (V2V) and vehicle to infrastructure (V2I) communication technologies on reducing potential crash risks during an emergency evacuation. Finally, as we have identified the limitations of simulation experiments, field experiments are necessary before deploying the recommendation in real-world hurricane evacuation.

## **6 Acknowledgments**

This research was supported by Safety Research Using Simulation (SAFER-SIM), University Transportation Center. We would like to thank Dr. Mohamed Abdel-Aty, Dr. Naveen Eluru, Dr. Mohamed H. Zaki, Dr. Qing Cai, and Dr. Yina Wu for their suggestions to this research, and Dawn Marshall and Jacob Heiden for providing oversight from SAFER-SIM.

## 7 References

1. Murray-Tuite, P., B. Wolshon, and D. Matherly. Evacuation and Emergency Transportation: Techniques and Strategies for Systems Resilience. *TR NEWS*, Vol. 311, 2017, p. 20.
2. Wu, Y., M. Abdel-Aty, and J. Lee. Crash Risk Analysis during Fog Conditions Using Real-Time Traffic Data. *Accident Analysis and Prevention*, Vol. 114, No. July 2016, 2018, pp. 4–11. <https://doi.org/10.1016/j.aap.2017.05.004>.
3. Tanishita, M., and B. van Wee. Impact of Vehicle Speeds and Changes in Mean Speeds on per Vehicle-Kilometer Traffic Accident Rates in Japan. *IATSS Research*, Vol. 41, No. 3, 2017, pp. 107–112. <https://doi.org/10.1016/j.iatssr.2016.09.003>.
4. Abdel-aty, M., N. Uddin, A. Pande, M. F. Abdalla, and L. Hsia. Predicting Freeway Crashes from Loop Detector Data by Matched Case-Control Logistic Regression. No. 1897, 2004, pp. 88–95.
5. Abdel-Aty, M. A., and H. T. Abdelwahab. Configuration Analysis of Two-Vehicle Rear-End Crashes. *Transportation Research Record: Journal of the Transportation Research Board*, Vol. 1840, No. 1, 2003, pp. 140–147. <https://doi.org/10.3141/1840-16>.
6. Kim, J.-K., Y. Wang, and G. F. Ulfarsson. Modeling the Probability of Freeway Rear-End Crash Occurrence. *Journal of Transportation Engineering*, Vol. 133, No. 1, 2007, pp. 11–19. [https://doi.org/10.1061/\(asce\)0733-947x\(2007\)133:1\(11\)](https://doi.org/10.1061/(asce)0733-947x(2007)133:1(11)).
7. Li, Y., Z. Li, H. Wang, W. Wang, and L. Xing. Evaluating the Safety Impact of Adaptive Cruise Control in Traffic Oscillations on Freeways. *Accident Analysis and Prevention*, Vol. 104, No. April, 2017, pp. 137–145. <https://doi.org/10.1016/j.aap.2017.04.025>.
8. Abdel-Aty, M., N. Uddin, and A. Pande. Split Models for Predicting Multivehicle

- Crashes During High-Speed and Low-Speed Operating Conditions on Freeways. *Transportation Research Record: Journal of the Transportation Research Board*, Vol. 1908, No. 1908, 2005, pp. 51–58. <https://doi.org/10.3141/1908-07>.
9. Zheng, Z., S. Ahn, and C. M. Monsere. Impact of Traffic Oscillations on Freeway Crash Occurrences. *Accident Analysis and Prevention*, Vol. 42, No. 2, 2010, pp. 626–636. <https://doi.org/10.1016/j.aap.2009.10.009>.
  10. Xu, C., P. Liu, W. Wang, and Z. Li. Evaluation of the Impacts of Traffic States on Crash Risks on Freeways. *Accident Analysis and Prevention*, Vol. 47, 2012, pp. 162–171. <https://doi.org/10.1016/j.aap.2012.01.020>.
  11. REGIONAL INTEGRATED TRANSPORTATION INFORMATION SYSTEM: A Data-Driven Platform for Transportation Analysis, Monitoring, and Data Visualization. <https://www.ritis.org/traffic/>.
  12. Roy, K. C., and S. Hasan. *Modeling the Dynamics of Hurricane Evacuation Decisions from Real-Time Twitter Data*. 2019.
  13. Abdel-Aty, M., A. Pande, A. Das, and W. J. Knibbe. Assessing Safety on Dutch Freeways with Data from Infrastructure-Based Intelligent Transportation Systems. *Transportation Research Record: Journal of the Transportation Research Board*, Vol. 2083, No. 1, 2009, pp. 153–161. <https://doi.org/10.3141/2083-18>.
  14. Hossain, M., and Y. Muromachi. A Bayesian Network Based Framework for Real-Time Crash Prediction on the Basic Freeway Segments of Urban Expressways. *Accident Analysis and Prevention*, Vol. 45, 2012, pp. 373–381. <https://doi.org/10.1016/j.aap.2011.08.004>.
  15. Lee, C., B. Hellinga, and F. Saccomanno. Real-Time Crash Prediction Model for Application to Crash Prevention in Freeway Traffic. *Transportation Research Record: Journal of the Transportation Research Board*, Vol. 1840, No. 1, 2003, pp. 67–77. <https://doi.org/10.3141/1840-08>.
  16. Krajzewicz, D. Traffic Simulation with SUMO – Simulation of Urban Mobility.

- International Series in Operations Research and Management Science*, Vol. 145, 2010, pp. 269–293. [https://doi.org/10.1007/978-1-4419-6142-6\\_7](https://doi.org/10.1007/978-1-4419-6142-6_7).
17. Kraus, S. *Microscopic Modeling Of Traffic Flow: Investigation of Collision Free Vehicle Dynamics*. Doctoral dissertation, Dt. Zentrum für Luft-und Raumfahrt eV, Abt. Unternehmensorganisation und-information, 1998.
  18. Kanagaraj, V., G. Asaithambi, C. H. N. Kumar, K. K. Srinivasan, and R. Sivanandan. Evaluation of Different Vehicle Following Models Under Mixed Traffic Conditions. *Procedia - Social and Behavioral Sciences*, Vol. 104, 2013, pp. 390–401. <https://doi.org/10.1016/j.sbspro.2013.11.132>.
  19. Milanés, V., and S. E. Shladover. Modeling Cooperative and Autonomous Adaptive Cruise Control Dynamic Responses Using Experimental Data. *Transportation Research Part C: Emerging Technologies*, Vol. 48, 2014, pp. 285–300. <https://doi.org/10.1016/j.trc.2014.09.001>.
  20. Treiber, M., and A. Kesting. Traffic Flow Dynamics Chp 11 Car-Following Models Based on Driving Strategies. In *Traffic Flow Dynamics*, Springer, pp. 181--204.
  21. Krajzewicz, D., G. Hertkorn, and P. Wagner. An Example of Microscopic Car Models Validation Using the Open Source Traffic Simulation SUMO. *Proceedings of Simulation in Industry 14th European Simulation Symposium*, 2002, pp. 318–322.
  22. Simulation of Urban Mobility: Vehicle Type Parameter Defaults. [https://sumo.dlr.de/docs/Vehicle\\_Type\\_Parameter\\_Defaults.html](https://sumo.dlr.de/docs/Vehicle_Type_Parameter_Defaults.html). Accessed May 7, 2019.
  23. Xiao, L., M. Wang, and B. van Arem. Realistic Car-Following Models for Microscopic Simulation of Adaptive and Cooperative Adaptive Cruise Control Vehicles. *Transportation Research Record: Journal of the Transportation Research Board*, Vol. 2623, No. 1, 2017, pp. 1–9. <https://doi.org/10.3141/2623-01>.
  24. Simulation of Urban Mobility: Car-Following-Models/ACC.

- <https://sumo.dlr.de/docs/Car-Following-Models/ACC.html>. Accessed Jun. 7, 2019.
25. Bash, E. The GEH Measure and Quality of the Highway Assignment M. European Transport Conference, Glasgow, Scotland, 1, 2012, pp. 42–50.
  26. Nezamuddin, N., N. Jiang, T. Zhang, and S. T. Waller. Traffic Operations and Safety Benefits of Active Traffic Strategies on Txdot Freeways. Vol. 7, No. Publication Number: FHWA. TX-12/0-6576-1, USA., 2011.
  27. Hayward, J. C. Near-Miss Determination through Use of a Scale of Danger. *Highway Res. Rec.*, Vol. 384, 1972, pp. 22–34.
  28. Wang, J., and R. Rajamani. The Impact of Adaptive Cruise Control Systems on Highway Safety and Traffic Flow. *Proceedings of the Institution of Mechanical Engineers, Part D: Journal of Automobile Engineering*, Vol. 218, No. 2, 2004, pp. 111–130. <https://doi.org/10.1243/095440704772913918>.
  29. Li, Y., L. Xing, W. Wang, H. Wang, C. Dong, and S. Liu. Evaluating Impacts of Different Longitudinal Driver Assistance Systems on Reducing Multi-Vehicle Rear-End Crashes during Small-Scale Inclement Weather. *Accident Analysis and Prevention*, Vol. 107, No. August, 2017, pp. 63–76.  
<https://doi.org/10.1016/j.aap.2017.07.014>.
  30. Li, Y., H. Wang, W. Wang, L. Xing, S. Liu, and X. Wei. Evaluation of the Impacts of Cooperative Adaptive Cruise Control on Reducing Rear-End Collision Risks on Freeways. *Accident Analysis and Prevention*, Vol. 98, 2017, pp. 87–95.  
<https://doi.org/10.1016/j.aap.2016.09.015>.
  31. Liu, H., X. (David) Kan, S. E. Shladover, X. Y. Lu, and R. E. Ferlis. Modeling Impacts of Cooperative Adaptive Cruise Control on Mixed Traffic Flow in Multi-Lane Freeway Facilities. *Transportation Research Part C: Emerging Technologies*, Vol. 95, No. July, 2018, pp. 261–279.  
<https://doi.org/10.1016/j.trc.2018.07.027>.
  32. Guo, Y., M. Essa, T. Sayed, M. M. Haque, and S. Washington. A Comparison

- between Simulated and Field-Measured Conflicts for Safety Assessment of Signalized Intersections in Australia. *Transportation Research Part C: Emerging Technologies*, Vol. 101, No. October 2018, 2019, pp. 96–110.  
<https://doi.org/10.1016/j.trc.2019.02.009>.
33. Essa, M., and T. Sayed. Transferability of Calibrated Microsimulation Model Parameters for Safety Assessment Using Simulated Conflicts. *Accident Analysis and Prevention*, Vol. 84, 2015, pp. 41–53.  
<https://doi.org/10.1016/j.aap.2015.08.005>.
34. Van Der Horst, R., and J. Hogema. Time-to-Collision and Collision Avoidance Systems. *proceedings of The 6th Workshop of the International*, 1993, pp. 1–12.
35. Cooper, D. F., and N. Ferguson. Traffic Studies at T-Junctions. 2. A Conflict Simulation Record. *Traffic Engineering & Control*, Vol. 17, No. Analytic, 1976.
36. *A Policy on Geometric Design of Highways and Streets*. American Association of State Highway and Transportation Officials, 2011.
37. Jeffery Archer. *Indicators for Traffic Safety Assessment and Prediction and Their Application in Micro-Simulation Modelling: A Study of Urban and Suburban Intersections*. KTH Royal Institute of Technology, 2005.
38. Simulation of Urban Mobility: Simulation/Output/SSM Device.  
[https://sumo.dlr.de/docs/Simulation/Output/SSM\\_Device.html](https://sumo.dlr.de/docs/Simulation/Output/SSM_Device.html). Accessed May 7, 2019.
39. Porfyri, K. N., E. Mintsis, and E. Mitsakis. Assessment of ACC and CACC Systems Using SUMO. Vol. 2, No. June, 2018, pp. 82–69.  
<https://doi.org/10.29007/r343>.